Electronic Supplementary Material (ESI) for Materials Chemistry Frontiers.
This journal is © the Partner Organisations 2022

Supplementary information

The scintillation properties of the HPS powder

The X-ray-excited luminescence (XRL) spectrum and scintillation decay profile of the HPS powder put up to a height of 7 mm in a quartz cell with inner dimensions of 10 mm× 44 mm × 1.0 mm (side dimensions of 12 mm × 45 mm × 3.5 mm) were measured. Fig. S1 (a) shows the XRL spectra of the HPS crystal and powder. The HPS powder in quartz cell exhibited an emission peak at approximately 480 nm. The emission peak of the HPS crystal appears at a slightly longer wavelength side than that of the HPS powder due to the self-absorption. Fig. S1 (b) shows the scintillation decay profile of the HPS powder for 511 keV γ-rays from ^{22}Na. The initial scintillation decay behavior of the HPS powder is distorted by Cherenkov radiation in the quartz cell. The scintillation decay profile of the HPS powder was approximated using the sum of two exponential functions. Table S1 shows the scintillation decay time constants of the HPS crystal and powder. The HPS powder exhibited the decay time constants of 5.2 and 16 ns. The decay time constant of 5.2 ns corresponds to the decay time constants of the first components of the HPS crystal. The decay time constant of 16 ns corresponds to the decay time constant of the second component of the HPS crystal. The HPS crystal exhibited the longer decay time constants than those of the HPS powder possibly due to self-absorption.

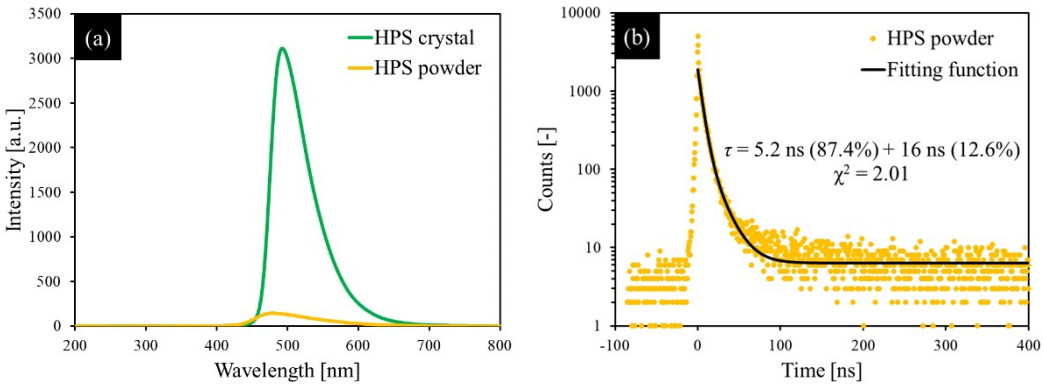

Fig. S1 (a) XRL spectra of the HPS crystal and powder, and (b) Scintillation decay profile of the HPS powder for 511 keV γ-rays from ^{22}Na.

Table S1 Scintillation decay time constants of HPS powder and crystal.

Sample	Decay time constant [ns]		χ^2
	First component	Second component	
Powder	5.2 (87.4%)	16 (12.6%)	2.01
Crystal	5.4 (94.6%)	21 (5.4%)	2.46

The size dependency of the scintillation properties

The scintillation properties were not correlated with the size of HPS crystal. We investigated the size dependency of the scintillation properties. Fig. S2 (a) shows the XRL spectra of the HPS crystals with thicknesses of 1.14, 1.28, and 1.32 mm. All the HPS crystals exhibited emission peaks at 490 nm. Fig. S2 (b) shows the pulse height spectra of the scintillation detectors equipped with the HPS crystals and EJ-256 for 67.41 keV X-rays. The photo-peak channel numbers obtained for the HPS crystals with thicknesses of 1.14, 1.28, and 1.32 mm were 280, 251, and 268, respectively. The variation of the obtained photo-peak channel numbers was within approximately 5%. The photo-peak channel position was not correlated within the thickness range of 1.14–1.32 mm. The size dependency of the scintillation properties was not observed in Fig. S2 (a) and (b).

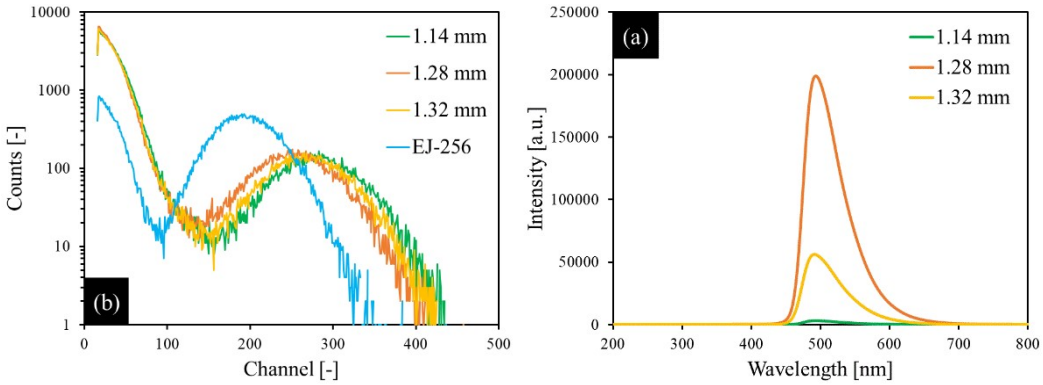

Fig. S2 (a) XRL spectra of HPS crystals with thicknesses of 1.14, 1.28, and 1.32 mm, and (b) Pulse height spectra of the scintillation detectors equipped with the HPS crystals and EJ-256 for 67.41 keV X-rays.

The responsiveness and cyclicity

Fig. S3 shows the change in X-ray-excited radioluminescence intensity at 490 nm of the HPS crystal for the number of X-ray irradiations. The XRL intensity at 490 nm decreased with an increase in the number of X-ray irradiation due to the radiation damage.

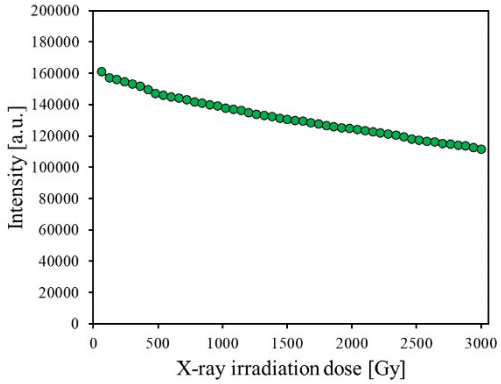

Fig. S3 Change in X-ray-excited radioluminescence intensity at 490 nm of the HPS crystal for the number of X-ray irradiations (the bias voltage of 40 kV and tube current of 40 mA).

The radio-stability under α- and X-ray irradiation

The HPS crystal scintillators are assumed to be used in not current mode detectors but pulse counting detectors, because current mode detectors do not require a fast scintillation decay time of nanoseconds. The lowest detection line for α- and X-ray of HPS crystals as current mode detectors is difficult to be measured. The radio-stability under α- and X-ray irradiation was evaluated measuring the pulse height spectra of the scintillation detectors equipped with the HPS crystal after α- and X-ray irradiation at different doses, respectively. Fig. S4 shows the pulse height spectra of the scintillation detectors equipped with the HPS crystal after α-ray irradiation at different doses (0–10 kGy) for 5.5 MeV α-rays from ^{241}Am. The photo-peak channel positions obtained for the HPS crystal were hardly changed after α-ray irradiation at 0, 1, and 10 kGy. Fig S5 shows the pulse height spectra of the scintillation detectors equipped with the HPS crystal after X-ray irradiation at different doses (0–10 kGy) for 59.5 keV γ-rays from ^{241}Am. The photo-peak channel numbers obtained for the HPS crystal after X-ray irradiation at 0, 1, and 10 kGy were 384, 385, and 327, respectively. According to this result, the reduction in the light yield were observed after X-ray irradiation at 10 kGy.

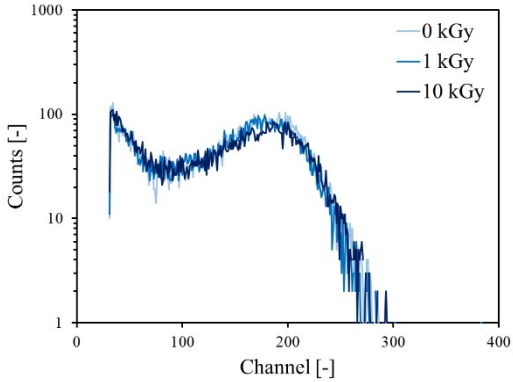

Fig. S4 Pulse height spectra of the scintillation detectors equipped with the HPS crystal after α-ray irradiation at different doses (0–10 kGy) for 5.5 MeV α-rays from ^{241}Am.

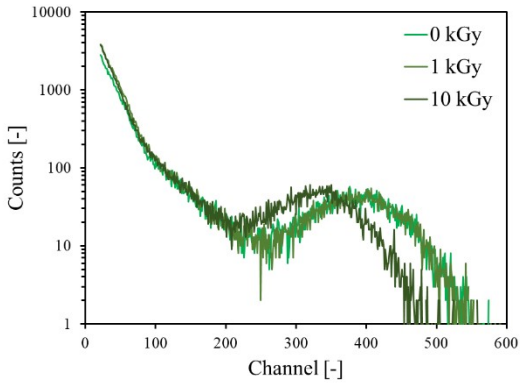

Fig. S5 Pulse height spectra of the scintillation detectors equipped with the HPS crystal after X-ray irradiation at different doses (0–10 kGy) for 59.5 keV γ-rays from ^{241}Am.